

Dual-Tone Radio Interferometric Positioning Systems Using Undersampling Techniques

Yiyin Wang¹, Li'an Li¹, Xiaoli Ma², Marie Shinotsuka², Cailian Chen¹ and Xiping Guan¹

¹ Department of Automation, Shanghai Jiao Tong University, Shanghai, 200240, China

² School of Electrical & Computer Engineering, Georgia Institute of Technology, Atlanta, GA 30332-0250, USA

Abstract—High accuracy and low cost are challenging requirements for localization in wireless sensor networks (WSNs). The radio interferometric positioning system (RIPS) proposed in [1] aims to meet both requirements at the same time. However, it is vulnerable to channel fading, and suffers from the noise aggravation due to the square operation. In this paper, we propose a dual-tone radio interferometric positioning system (DRIPS) using undersampling techniques, named uDRIPS. Our proposed methodology is immune to flat fading effects, and avoids the amplification of measurement noise by directly undersampling the received signal. Furthermore, the time-of-arrival (TOA) information is extracted from the phases of the received dual-tone signals in the uDRIPS. As a result, it is able to localize an asynchronous target with the help of synchronous anchors (nodes with known positions). Moreover, we investigate the integer ambiguity problem due to phase wrapping, and develop a localization algorithm to estimate the unknowns alternatively. Simulation results corroborate the efficiency of our proposed algorithm.

Index Terms—Ranging, radio interferometric positioning, localization, undersampling

EDICS: SAM-LOC, Sensor network localization algorithms.

I. INTRODUCTION

Accurate and low-cost localization is a critical task for wireless sensor networks (WSNs). The data collected by sensors need to be associated with location information [2], [3]. The low-cost constraint of sensor nodes calls for low-complexity localization methods while the high accuracy requirement makes the localization task challenging. Although the unique properties of ultra-wideband (UWB) impulse radio (IR) [4], [5] promote time-based localization with high accuracy, the prohibitively high Nyquist rate and hardware requirement of UWB systems hinder their popularity. Hence, we concentrate on narrowband localization systems to increase the localization accuracy.

A radio interferometric positioning system (RIPS) is proposed in [1] to achieve both high accuracy and low cost. The ranging principle of the RIPS can be exemplified for synchronous nodes. Two transmitters emit two sinusoid signals of slightly different frequencies denoted by $a_1 \cos(2\pi f_1 t)$ and $a_2 \cos(2\pi f_2 t)$, respectively, where a_1 and a_2 are real-valued amplitudes, and f_1 and f_2 the frequencies with

$f_1, f_2 \gg |f_1 - f_2|$. A receiver creates a low-frequency differential signal by low-pass filtering (denoted by $\text{LPF}\{\cdot\}$) the received signal strength indicator (RSSI) signal as

$$\begin{aligned} & \text{LPF}\{r^2(t)\} \\ &= \text{LPF}\{(a_1 \cos(2\pi f_1(t - \tau_1)) + a_2 \cos(2\pi f_2(t - \tau_2)) + n(t))^2\} \\ &= (a_1^2 + a_2^2)/2 + a_1 a_2 \cos(2\pi(f_1 - f_2)t + 2\pi(f_2 \tau_2 - f_1 \tau_1)) + \tilde{n}(t), \end{aligned}$$

where $r(t)$ is the received signal, τ_1 and τ_2 are the propagation delays, $n(t)$ is the noise term, and $\tilde{n}(t)$ is the aggregate noise term including the noise autocorrelation and signal-noise cross-correlation terms. Thus, $\tilde{n}(t)$ has a higher variance than $n(t)$. Note that the phase of the low-frequency differential signal ($a_1 a_2 \cos(2\pi(f_1 - f_2)t + 2\pi(f_2 \tau_2 - f_1 \tau_1))$) bears the range information. Nevertheless, the RIPS only accommodates additive white Gaussian noise (AWGN) channels, suffers from the increased noise due to the square operation, and faces the integer ambiguity issue.

The RIPS is further extended in [6], [7] to track mobile nodes, where Doppler shifts are exploited such that velocity estimates of moving targets can be achieved. Moreover, spinning anchors transmitting radio signals with fixed frequencies (SpinLoc) are proposed in [8] to produce specified Doppler signals in order to estimate angle-of-arrivals (AOAs). Software defined radios are used to implement interferometric localization with the assistance of AOAs in [9]. The FPGA implementation of the RIPS is investigated in [10] to provide a more robust and flexible platform. A stochastic RIPS (SRIPS) is developed in [11] to make use of radios at 2.4 GHz. An asynchronous RIPS (ARIPS) is proposed in [12], where dual-tone signals from separate nodes are employed to localize asynchronous targets. However, the ARIPS is still designed for AWGN channels. More recently, a dual-tone radio interferometric positioning system (DRIPS) for multi-target localization is developed in [13] to combat the flat-fading channel. It employs a square-law device similar to the RIPS to produce a low-frequency differential signal, and thus suffers from high noise power and not-so-flexible hardware design (e.g., the choice of sampling rate).

In this letter, we introduce an undersampling technique to DRIPS, and name it as uDRIPS. It inherits the dual-tone signal structure of the DRIPS, but does not employ the square-law device. Hence, uDRIPS maintains all the advantages of the DRIPS, but does not introduce noise multiplication terms. Therefore, uDRIPS avoids noise amplification. Different from the dual-tone signals of the ARIPS, the two tones of the dual-

Part of this work was supported by the National Nature Science Foundation of China (No. 61301223, No. 61174127, No. 61221003 and No. 61273181), the Nature Science Foundation of Shanghai (No. 13ZR1421800), and the Georgia Tech Ultra-wideband Center of Excellence (<http://www.uwbtech.gatech.edu/>).

tone signal in the uDRIPS are close to each other in frequency. Moreover, their frequency difference is designed to be smaller than the channel coherence bandwidth. Therefore, the uDRIPS is robust to flat-fading channels. Given the freedom of the target clock, the time-of-arrival (TOA) plus an offset due to the unknown transmission time can be extracted from the phases of the dual-tone signals in the uDRIPS. Hence, our proposed algorithm is able to localize an asynchronous target with the assistance of synchronous anchors. Furthermore, we explore the integer ambiguity problem due to phase wrapping, and develop a localization algorithm to find the unknowns alternatively. Simulations demonstrate the promising performance of the proposed system.

II. SYSTEM MODEL

Let us consider a scenario where a single target is to be localized by communicating with M anchors with known positions. The target transmits a dual-tone signal

$$s(t) = ae^{j\varphi} e^{j2\pi(f_c+f_b)(t-t_0)}(1 + e^{j2\pi g_b(t-t_0)}), \quad (1)$$

where a is the real-valued amplitude of each of the components, φ is the unknown initial phase offset, f_c is the carrier frequency, f_b is the frequency of the first tone component and greater than zero, g_b is the small frequency difference between the two tones and greater than zero as well, and t_0 is the unknown time instant when the target starts to transmit. The following assumptions are adopted throughout the paper.

Assumption 1: All M anchors are assumed to be synchronized, but the target clock can run independently.

Assumption 2: The unknown t_0 is due to the lack of synchronization between the target and the anchors, and thus it introduces an unknown phase offset between the two tones. Since M anchors are synchronized, the unknown t_0 is assumed to be the same with respect to (w.r.t.) all the anchors.

Assumption 3: The frequency difference g_b is assumed to be smaller than the channel coherence bandwidth. As a result, the two tones of the dual-tone signal experience the same channel fading effect [14], and a flat-fading channel model is applied here to account for the fading effect.

With these assumptions, the signal received by the l th anchor is down converted by f_c , and then modeled as

$$r_l(t) = \beta_l s(t - \tau_l) e^{-j2\pi f_c t + j\eta_l} + w_l(t), \quad (2)$$

where β_l is a complex channel coefficient attributing to the flat-fading channel effects, and can be modeled as a zero-mean complex Gaussian random variable with variance σ_l^2 representing the average power of the flat-fading channel. Moreover, τ_l is the unknown propagation delay, d_l is the distance between the target and the l th anchor, and $d_l = \nu\tau_l$, where ν is the signal propagation speed. The unknown initial phase η_l is due to the randomness of the receiver oscillator. Furthermore, the noise term $w_l(t)$ is modeled as a zero-mean complex Gaussian random process with variance σ^2 . Substituting (1) into (2), we obtain

$$r_l(t) = \alpha_l \beta_l e^{j2\pi f_b t} e^{j\theta_l} (1 + e^{j2\pi g_b t} e^{j\phi_l}) + w_l(t), \quad (3)$$

where $\theta_l = -2\pi(f_c + f_b)(t_0 + \tau_l)$, $\phi_l = -2\pi g_b(t_0 + \tau_l)$, and $\alpha_l = ae^{j(\varphi + \eta_l)}$ is an aggregate complex parameter to absorb

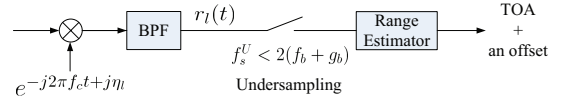


Fig. 1. The receiver structures of the uDRIPS.

the effects of the random initial phases between the target and the l th anchor. Note that ϕ_l includes the range of interest (via τ_l). Although we only consider a single target scenario, the uDRIPS can be adapted for a multi-target scenario similarly as the DRIPS.

III. RANGE ESTIMATION

In this section, we propose a ranging method for the uDRIPS, and investigate the integer ambiguity problem.

A. uDRIPS: Range Estimation With Undersampling

The receiver structure of the uDRIPS is shown in Fig.1, where the received signal is down converted, bandpass filtered, and directly undersampled. Since the bandwidth of each component of $r_l(t)$ is much less than the frequency difference g_b of the two components and only the phases of these tone components but not their frequencies are of interest, we can make use of the undersampling technique. The reason to employ the undersampling technique is two-fold: i) to simplify the receiver structure, and ii) to avoid amplifying the noise. As a result, the square-law device is removed and no noise autocorrelation or signal-noise cross-correlation terms are generated in the uDRIPS compared to the DRIPS and RIPS. Note that the down conversion is necessary to facilitate the design of the bandpass filter (BPF) and the employment of analog-to-digital convertor (ADC). The BPF, whose center frequency is $f_b + g_b/2$ and bandwidth is greater than g_b , is designed to suppress the interference due to undersampling. The frequency down conversion also helps to choose the ADC since the high frequency and bandwidth require high accuracy of the sampling clock and hardware.

At the receiver, the signal $r_l(t)$ in (3) is undersampled at the rate f_s^U directly, where $f_s^U < 2(f_b + g_b)$. For the sake of brevity, the noise term is neglected from now on. Collecting all L samples into a vector \mathbf{r}_l^U , we arrive at

$$\mathbf{r}_l^U = \mathbf{A}_L^U \mathbf{x}_l^U, \quad (4)$$

where $\mathbf{x}_l^U = \alpha_l \beta_l [e^{j\theta_l}, e^{j(\theta_l + \phi_l)}]^T$, and $\mathbf{A}_L^U = [\Phi_L(f_b/f_s^U) \Phi_L((f_b + g_b)/f_s^U)]$ with $\Phi_L(f) = [1, e^{j2\pi f}, \dots, e^{j2\pi(L-1)f}]^T$. Consequentially, a least-squares (LS) estimator of \mathbf{x}_l^U is given by

$$\hat{\mathbf{x}}_l^U = (\mathbf{A}_L^U)^\dagger \mathbf{r}_l^U, \quad (5)$$

and the phase of interest ϕ_l can be estimated as

$$\hat{\phi}_l = \arg \{ [\hat{\mathbf{x}}_l^U]_1^* [\hat{\mathbf{x}}_l^U]_2 \} + 2\pi k, \quad (6)$$

where $[\mathbf{a}]_n$ denotes the n th entry of the vector \mathbf{a} , the unknown integer k accounts for the integer ambiguity due to phase wrapping, and $(\cdot)^*$ denotes the complex conjugate. Using $\hat{\phi}_l$ in (6), the TOA with an offset due to the unknown transmission time t_0 can be estimated. However, the integer ambiguity issue has to be considered in the TOA estimation. More details about

the integer ambiguity issue will be discussed in Section III-B. Several remarks are now due.

Remark 1: The unknown phase shift (θ_l), the effects of the random initial phases (α_l), and the flat-fading channel (β_l) are absent in (6). Hence, the uDRIPS is immune to the uncertainty of the initial phases and the flat-fading effect. In this case, uDRIPS is a non-coherent localizer.

Remark 2: The clock of the target does not have to be synchronized with the anchor clocks. New targets can enter the network and can be localized at any time.

Remark 3: The main sources of ranging errors are due to the lack of time and frequency synchronization among the anchors. The time synchronization among the anchor receivers can be accomplished by various approaches [15], [16]. For example, using the method proposed in [16], the average time synchronization error can be below $1 \mu\text{s}$. As a result, the phase error is less than $10^{-6} \cdot 2\pi g_b$. Furthermore, the frequencies of the two tones ($f_b + g_b$ and f_b) in (3) may not be exactly known due to oscillator uncertainties of the target transmitter or the anchor receivers. In this situation, these frequencies can be estimated similarly by the ESPRIT-type method proposed in the ARIPS (see [12]), and then the phases is extracted using the estimated frequencies. Assuming a frequency estimation error Δf , it would be translated as an additional phase estimation error ($-2\pi\Delta f(t_0 + \tau_l)$).

Remark 4: The choice of f_s^U is critical in the uDRIPS. It should fulfill the conditions that

$$f_s^U \neq g_b/n_1 \text{ and } f_s^U \neq f_b/n_2, \quad (7)$$

where $n_1, n_2 \in \mathcal{Z}^+$ and \mathcal{Z}^+ includes all positive integers. In order to extract the phase information of the two tones, the tones should not alias with each other and do not reduce to DC components after undersampling. This leads us to the condition imposed by (7). Furthermore, the lower the undersampling rate f_s^U is, the smaller the burden is for the digital signal processing part of the receivers. On the other hand, the lower the undersampling rate f_s^U is, the fewer samples are collected in a fixed time duration resulting in the degradation of the estimation accuracy. Therefore, there is a tradeoff for the selection of f_s^U .

B. Integer Ambiguity Issue

As we observe from (6), the true ϕ_l cannot be calculated because of the unknown integer k . This is the well-known integer ambiguity problem due to phase wrapping [17], [18]. Hence, we can only obtain $\hat{\hat{\phi}}_l$ ($\hat{\hat{\phi}}_l = \arg\{[\hat{\mathbf{x}}_l^U]^*[\hat{\mathbf{x}}_l^U]\}$) instead of $\hat{\phi}_l$ from (6), where $\hat{\hat{\phi}}_l$ is the estimate of $\tilde{\phi}_l$ and $\phi_l = \tilde{\phi}_l + 2\pi k$. Recall that τ_l is coupled with t_0 as $\phi_l = -2\pi g_b(t_0 + \tau_l)$. Hence, we can obtain the estimate of the TOA plus an offset, called the biased TOA as

$$\hat{t}_0 + \hat{\tau}_l = -(\hat{\hat{\phi}}_l/2\pi + k)/g_b. \quad (8)$$

Let us define $\delta_0 = -2\pi g_b t_0$ and $\tilde{\delta}_0 = \delta_0 - 2\pi[\delta_0/2\pi]$, $\varepsilon_l = -2\pi g_b \tau_l$ and $\tilde{\varepsilon}_l = \varepsilon_l - 2\pi[\varepsilon_l/2\pi]$. As

$$[\phi_l/2\pi] = \begin{cases} \lfloor \delta_0/2\pi \rfloor + \lfloor \varepsilon_l/2\pi \rfloor & \text{if } 0 \leq \tilde{\delta}_0 + \tilde{\varepsilon}_l < 2\pi \\ \lfloor \delta_0/2\pi \rfloor + \lfloor \varepsilon_l/2\pi \rfloor + 1 & \text{if } 2\pi \leq \tilde{\delta}_0 + \tilde{\varepsilon}_l < 4\pi \end{cases}, \quad (9)$$

we arrive at

$$\tilde{\phi}_l = \begin{cases} \tilde{\delta}_0 + \tilde{\varepsilon}_l & \text{if } 0 \leq \tilde{\delta}_0 + \tilde{\varepsilon}_l < 2\pi \\ \tilde{\delta}_0 + \tilde{\varepsilon}_l - 2\pi & \text{if } 2\pi \leq \tilde{\delta}_0 + \tilde{\varepsilon}_l < 4\pi \end{cases}. \quad (10)$$

According to (10), $\tilde{\phi}_l$ is related to $\tilde{\delta}_0$ and $\tilde{\varepsilon}_l$ in two possible ways. In the next section, we will simplify the above integer ambiguity problem, and develop the corresponding localization method using the biased TOAs.

IV. LOCALIZATION ALGORITHM

In this section, a localization algorithm is proposed for the uDRIPS with a simplified integer ambiguity problem, which indicates that the phase shift ε_l ($\varepsilon_l = -2\pi g_b \tau_l$) is in the range of $(-2\pi, 0)$ ($-2\pi < \varepsilon_l < 0$). Hence, the corresponding distance d_l ($d_l = \nu \tau_l$) is in the range of $(0, \nu/g_b)$, which is called the resolvable range, and the distance d_l in the resolvable range can be estimated without ambiguity. The smaller the frequency difference g_b is, the larger the resolvable range is. It also ensures that two tones experience the same channel fading effect. However, a larger frequency difference g_b facilitates a higher estimation accuracy. Therefore, there is a tradeoff in designing g_b . According to the range of ε_l ($-2\pi < \varepsilon_l < 0$), we achieve $[\varepsilon_l/2\pi] = -1$ and $\tilde{\varepsilon}_l = \varepsilon_l + 2\pi$. We can rewrite (10) in the relation w.r.t. d_l as

$$-\frac{\tilde{\phi}_l \nu}{2\pi g_b} = \begin{cases} b_0 + d_l - \nu/g_b & \text{if } 0 \leq \tilde{\delta}_0 + \varepsilon_l < 2\pi \\ b_0 + d_l & \text{if } 2\pi \leq \tilde{\delta}_0 + \varepsilon_l < 4\pi \end{cases}, \quad (11)$$

where $b_0 = -\nu\tilde{\delta}_0/2\pi g_b$ is the distance offset due to the unknown transmission time.

Let us collect all the phase estimates $\hat{\hat{\phi}}_l$ into a vector \mathbf{v} as $\mathbf{v} = -(\nu/2\pi g_b)[\hat{\hat{\phi}}_0, \hat{\hat{\phi}}_1, \dots, \hat{\hat{\phi}}_{M-1}]^T$. Without the error term, the model of \mathbf{v} is given by

$$\mathbf{v} = \mathbf{d} + b_0 \mathbf{1}_M + (\nu/g_b)\mathbf{u}, \quad (12)$$

where $\mathbf{d} = [d_0, d_1, \dots, d_{M-1}]^T$ with $d_l = \|s_l - \mathbf{x}\|$, s_l and \mathbf{x} denote the coordinates of the l th anchor and the target, respectively, and \mathbf{u} belongs to the set $\{0, -1\}^M$. The nonlinear relationship of (12) w.r.t. \mathbf{x} increases the difficulties in solving (12). An alternating least squares (ALS) solution [19] is employed here. The unknown parameters \mathbf{x} and b_0 are categorized as a subset, while \mathbf{u} is another subset. We define the estimates of the n th iteration as $\hat{\mathbf{x}}^{(n)}$, $\hat{b}_0^{(n)}$, and $\hat{\mathbf{u}}^{(n)}$. Let us assume the knowledge of $\hat{\mathbf{u}}^{(n-1)}$. Thus, we obtain a linear model w.r.t. \mathbf{x} and b_0 by moving $(\nu/g_b)\hat{\mathbf{u}}^{(n-1)}$ and $b_0 \mathbf{1}_M$ to the left side of (12). After element-wise multiplication (denoted by \odot) and moving the unknowns (\mathbf{x} , $\|\mathbf{x}\|^2$ and b_0) to the left side, we obtain

$$\Phi - \tilde{\mathbf{v}}^{(n)} \odot \tilde{\mathbf{v}}^{(n)} = 2\mathbf{S}^T \mathbf{x} - 2b_0 \tilde{\mathbf{v}}^{(n)} + (b_0 - \|\mathbf{x}\|^2) \mathbf{1}_M, \quad (13)$$

where $\tilde{\mathbf{v}}^{(n)} = \mathbf{v} - (\nu/g_b)\hat{\mathbf{u}}^{(n-1)}$, $\mathbf{S} = [s_0 \ s_1 \ \dots \ s_{M-1}]$, and $\Phi = [\|s_0\|^2, \|s_1\|^2, \dots, \|s_{M-1}\|^2]^T$. As a result, the estimate of $\mathbf{x}^{(n)}$ and $b_0^{(n)}$ can be achieved based on (13) using an LS estimator [20]. Consequently, the update of $\hat{\mathbf{u}}^{(n)}$ can be employed by a simple rounding operation as

$$\hat{\mathbf{u}}^{(n)} = \begin{cases} 0 & \text{if } \text{round}\left(\frac{g_b}{\nu} \left(\mathbf{v} - \hat{\mathbf{d}}^{(n)} - \hat{b}_0^{(n)} \mathbf{1}_M\right)\right) \geq 0 \\ -1 & \text{if } \text{round}\left(\frac{g_b}{\nu} \left(\mathbf{v} - \hat{\mathbf{d}}^{(n)} - \hat{b}_0^{(n)} \mathbf{1}_M\right)\right) < 0 \end{cases}. \quad (14)$$

The ALS algorithm is summarized in Algorithm 1.

Algorithm 1: an ALS approach to localize the target

- 1) Initial step: $\hat{\mathbf{u}}^{(0)} = \mathbf{0}$
 - 2) Update $\hat{\mathbf{x}}^{(n)}$ and $\hat{b}_0^{(n)}$ given $\hat{\mathbf{u}}^{(n-1)}$ based on the linear model (13)
 - 3) Update $\hat{\mathbf{u}}^{(n)}$ given $\hat{\mathbf{x}}^{(n)}$ and $\hat{b}_0^{(n)}$ using (14)
 - 4) Go back to step 2), unless $\|\hat{\mathbf{x}}^{(n)} - \hat{\mathbf{x}}^{(n-1)}\| < \epsilon$ or reach the maximum iteration number
-

V. SIMULATION RESULTS

In this section, the performance of the uDRIPS is evaluated, and compared to the DRIPS in [12]. The frequency of the first component of the dual-tone signal $f_b = 5$ MHz, and the frequency difference $g_b = 50$ kHz, which is smaller than the typical channel coherence bandwidth 100 kHz according to the Extended Typical Urban (ETU) channel model in the 3GPP-LTE standard [21]. The observation duration is 5 milliseconds (ms). The amplitude of the dual-tone signal $a = 1$, and the carrier frequency $f_c = 2.45$ GHz. Moreover, the average channel power of the flat-fading channel is always assumed to be 1 for all channels, i.e., $\sigma_l^2 = 1, l = 0, \dots, M - 1$. The signal-to-noise ratio (SNR) is defined as $1/\sigma^2$, where σ^2 is the variance of the noise term $w_l(t)$. Furthermore, we assume that the target is in the range of the resolving limit ($0 < d_l < \nu/g_b = 6$ km with $\nu = 3 \times 10^8$ m/s). Thus, a simplified integer ambiguity problem is considered here. For each evaluation, 10,000 Monte-Carlo runs are carried out.

In Figs. 2 and 3, the ranging accuracy of the uDRIPS is compared to the DRIPS excluding the impact of the unknown transmission instant t_0 . Hence, we assume the target and the anchors are synchronized ($t_0 = 0$) in Figs. 2 and 3. Recall that the target is in the resolvable range. The true distance between the target and the anchor is set to be 1.2 km. In each Monte-Carlo run, the complex channel coefficient β_l ($\beta_l \sim \mathcal{CN}(0, 1)$) is generated randomly.

The root mean square error (RMSE) of the range estimate is shown in Fig. 2. The uDRIPS (the solid lines) employing undersampling frequencies that satisfy the condition imposed by (7) performs well (see $f_s^U = 15$ kHz and $f_s^U = 55$ kHz cases in Fig. 2), and the estimation accuracy increases with the increasing sampling frequency. However, for the sampling frequency of 25 kHz, the uDRIPS (the solid line with “+” markers) fails, since the condition imposed by (7) is violated. Note that for a given observation duration, the higher the frequency is, the more samples are obtained. With a half number of samples compared to the DRIPS, the ranging accuracy of the uDRIPS ($f_s^U = 55$ kHz) is still slightly better than the DRIPS ($f_s^D = 110$ kHz) at low SNR. This is because that the uDRIPS does not suffer from the noise aggravation due to the square operation used in the DRIPS.

The complementary cumulative distribution function (CCDF) curves of the absolute distance errors for the uDRIPS ($f_s^U = 55$ kHz) and the DRIPS ($f_s^D = 110$ kHz) are illustrated in Fig. 3, respectively, where $\text{SNR} = \{5 \text{ dB}, 25 \text{ dB}, 45 \text{ dB}\}$. Although the number of samples used in the DRIPS is two times of the one in the uDRIPS, the CCDF curves of the

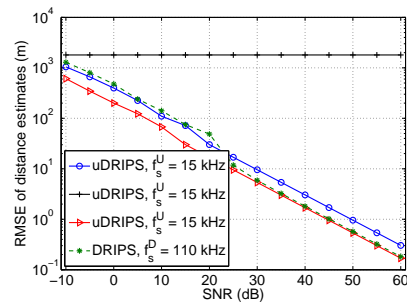


Fig. 2. RMSE of distance estimates vs. SNR

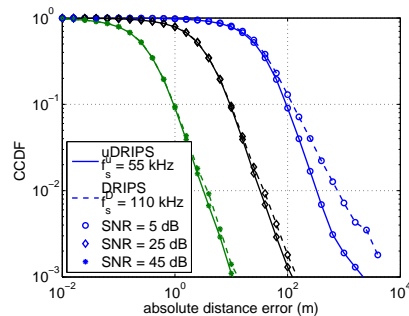


Fig. 3. The CCDF curves of the absolute distance errors at different SNRs for the uDRIPS ($f_s^U = 55$ kHz) and the DRIPS ($f_s^D = 110$ kHz)

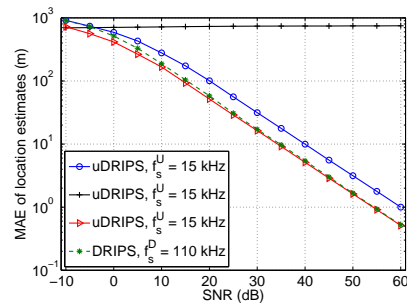


Fig. 4. MAE of location estimates vs. SNR

uDRIPS (the solid lines) are lower than the ones of the DRIPS (the dashed lines), and the differences increase as the SNR decreases. The noise amplification is significant at low SNR for the DRIPS.

Localization accuracy is evaluated with five anchors and a target. The target is not synchronized with anchors. Thus, the time instant t_0 is randomly generated in the range of $(0, 100] \mu\text{s}$ for each run. The coordinates for five anchors and the target are $\mathbf{s}_0 = [0, 1000 \text{ m}]^T$, $\mathbf{s}_1 = [1000 \text{ m}, 0]^T$, $\mathbf{s}_2 = [0, 0]^T$, $\mathbf{s}_3 = [1000 \text{ m}, 2000 \text{ m}]^T$, $\mathbf{s}_4 = [2000 \text{ m}, 1000 \text{ m}]^T$ and $\mathbf{x} = [1500 \text{ m}, 1200 \text{ m}]^T$, respectively. The median absolute error (MAE) is used as a performance metric in this simulation to mitigate the effects of the outliers due to the deep fading. The integer ambiguity issue is solved by the ALS approach proposed in Section IV. The localization accuracy is illustrated in Fig. 4 for both the uDRIPS and the DRIPS, where the uDRIPS ($f_s^U = 55$ kHz) slightly outperforms the DRIPS ($f_s^D = 110$ kHz) even with a half number of samples.

ACKNOWLEDGEMENT

The authors would like to thank Prof. G. Tong Zhou for insightful discussions.

REFERENCES

- [1] M. Maróti, P. Völgyesi, S. Dóra, B. Kusy, A. Nádas, Á. Lédéczi, G. Balogh, and K. Molnár, "Radio interferometric geolocation," in *Proc. ACM Sensys*, San Diego, USA, Nov. 2005, pp. 1–12.
- [2] N. Patwari, J. N. Ash, S. Kyperountas, A. O. Hero, R. L. Moses, and N. S. Correal, "Locating the nodes: cooperative localization in wireless sensor networks," *IEEE Signal Process. Mag.*, vol. 22, pp. 54–69, July 2005.
- [3] I. F. Akyildiz, W. Su, Y. Sankarasubramaniam, and E. Cayirci, "Wireless sensor networks: a survey," *Computer Networks*, vol. 38, pp. 393–422, Mar. 2002.
- [4] S. Gezici, Z. Tian, G. B. Giannakis, H. Kobayashi, A. F. Molisch, H. V. Poor, and Z. Sahinoglu, "Localization via ultra-wideband radios: a look at positioning aspects for future sensor networks," *IEEE Signal Process. Mag.*, vol. 22, pp. 70–84, July 2005.
- [5] Z. Sahinoglu, S. Gezici, and G. Ismail, *Ultra-wideband Positioning Systems*, vol. 2, Cambridge University Press Cambridge, UK, 2008.
- [6] B. Kusy, J. Sallai, G. Balogh, A. Lédéczi, V. Protopopescu, J. Tolliver, F. DeNap, and M. Parang, "Radio interferometric tracking of mobile wireless nodes," in *Proc. ACM MobiSys*, San Juan, Puerto Rico, June 2007, pp. 139–151.
- [7] B. Kusy, A. Lédéczi, and X. Koutsoukos, "Tracking mobile nodes using RF doppler shifts," in *Proc. ACM Sensys*, Sydney, Australia, Nov. 2007, pp. 29–42.
- [8] H. Chang, J. Tian, T. Lai, H. Chu, and P. Huang, "Spinning beacons for precise indoor localization," in *Proc. ACM SenSys*, Raleigh, USA, Nov. 2008, pp. 127–140.
- [9] J. Friedman, A. Davitian, D. Torres, D. Cabric, and M. Srivastava, "Angle-of-arrival-assisted relative interferometric localization using software defined radios," in *Proc. IEEE MILCOM*, Boston, USA, Oct. 2009, pp. 1–8.
- [10] S. Szilvasi, J. Sallai, I. Amundson, P. Volgyesi, and A. Lédéczi, "Configurable hardware-based radio interferometric node localization," in *Proc. IEEE Aerospace Conf.*, Big Sky, USA, Mar. 2010, pp. 1–10.
- [11] B. J. Dil and P. J. M. Havinga, "Stochastic radio interferometric positioning in the 2.4 GHz range," in *Proc. ACM SenSys*, Seattle, USA, Nov. 2011, pp. 108–120.
- [12] Y. Wang, M. Shinotsuka, X. Ma, and M. Tao, "Design an asynchronous radio interferometric positioning system using dual-tone signaling," in *Proc. IEEE WCNC*, Shanghai, China, Apr. 2013, pp. 2294 – 2298.
- [13] Y. Wang and X. Ma, "Designing dual-tone radio interferometric positioning systems," Tech. Rep., Georgia Institute of Technology, May 2013.
- [14] J. G. Proakis and M. Salehi, *Digital Communications*, vol. 3, McGraw-Hill New York, 2008.
- [15] Y.-C. Wu, Q. Chaudhari, and E. Serpedin, "Clock synchronization of wireless sensor networks," *IEEE Signal Process. Mag.*, vol. 28, no. 1, pp. 124–138, 2011.
- [16] F. Ferrari, M. Zimmerling, L. Thiele, and O. Saukh, "Efficient network flooding and time synchronization with Glossy," in *Proc. IEEE IPSN*, Chicago, USA, Apr. 2011, pp. 73–84.
- [17] P. J. G. Teunissen, "The least-squares ambiguity decorrelation adjustment: a method for fast GPS integer ambiguity estimation," *Journal of Geodesy*, vol. 70, pp. 65–82, Nov. 1995.
- [18] P. J. G. Teunissen, P. J. de Jonge, and C. C. J. M. Tiberius, "The least-squares ambiguity decorrelation adjustment: its performance on short GPS baselines and short observation spans," *Journal of Geodesy*, vol. 71, pp. 589–602, Sept. 1997.
- [19] Y. Takane, F. W. Young, and J. De Leeuw, "Nonmetric individual differences multidimensional scaling: an alternating least squares method with optimal scaling features," *Psychometrika*, vol. 42, pp. 7–67, Mar. 1977.
- [20] Y. Wang and G. Leus, "Reference-free time-based localization for an asynchronous target," *EURASIP Journal on Advances in Signal Processing*, vol. 2012, pp. 1–21, Jan. 2012.
- [21] H. G. Myung, "Technical overview of 3GPP LTE," *Polytechnic University of New York*, 2008.